Ruling uncertainties in Range-only Robot Localisation

Farhad Shamsfakhr
University of Trento - Dep. of Industrial Engineering
Trento, Italy
Email: farhad.shamsfakhr@unitn.it

Luigi Palopoli
University of Trento - Dep. of Eng. and Computer Science
Trento, Italy
Email: luigi.palopoli@unitn.it

David Macii
University of Trento - Dep. of Industrial Engineering
Trento, Italy
Email: david.macii@unitn.it

Daniele Fontanelli
University of Trento - Dep. of Industrial Engineering
Trento, Italy
Email: daniele.fontanelli@unitn.it

***Abstract*—We consider a mobile robot localising itself through a set of UWB wireless anchors. We show how the use of an appropriate localisation algorithm allows for an analytical estimate of the localisation uncertainty. This information is used to build a potential-based motion planning algorithm that drives the robot along trajectories, while achieving a good tradeoff between moving toward the goal and keeping localisation uncertainty reasonably low.**

***Index Terms*—Range-only Measurements, Localisation, Uncertainty Analysis, Uncertainty Control**

I. Introduction

In modern industrial practice, mobile robots are prominently used for moving goods between different areas of the factory. In crowded or cluttered environments, especially when robots have to interact closely with human operators, high levels of robot autonomy are needed in decided the path to follow to reach a given destination. This scenario is technologically challenging and requires a very high localisation accuracy all over the robot mission. In this paper, we consider the case in which the robot planar position and orientation is estimated through he fusion of dead-reckoning (e.g., using encoders installed on robots' wheels) and distance measurement data from a set of external wireless nodes (briefly referred to as "anchors" in the following) with known coordinates in a given reference frame. In particular, since the localisation uncertainty depends on the relative positions of the robot and the detectable anchors, our idea is to account for localisation uncertainty when deciding a motion plan. In other words, the while reaching the destination, a robot should move along the path that minimises the localisation uncertainty.

The problem of robot localisation has received a constant attention over the last few years. In the wide range of technological options explored in the past to estimate the position of mobile robots, it is possible to mention fingerprinting of Wi-Fi signals [2], detection of radio frequency identification (RFID) tags [3], [4], computer vision techniques using both natural [5] and artificial landmarks [6], [7], and Light Detection and Ranging (LiDAR) sensors [8]. Particularly relevant to this paper are the multilateration solutions that exploit the distance of the robot from a set of fixed wireless anchors placed at known coordinates [9]. The distance values between the wireless transceiver installed on the robot and the anchors can be estimated indirectly from the Received Signal Strength Indication (RSSI) values [10], [11] or through the Time-of-Arrival (ToA), the Time-Difference-of-Arrival (TDoA) or Round-Trip Time (RTT) measurement of messages exchanged between pairs of wireless devices. In this respect, the use of Ultra-Wideband (UWB) signals ensures a very high ranging accuracy, at least in Line-of-Sight conditios (i.e., a few centimetres instead of of one or more metres, as it results if RSSI or TDoA measurements from Wi-Fi devices are performed) [1]. The recent availability of new-generation, smaller and low-cost UWB transceivers offering decimetre-level accuracy (e.g., the DecaWave DW1000 [12]) has lowered the adoption barriers for this technology.

When fixed anchors are used, one of the key challenges is how to reconcile a high level of accuracy with the deployment and maintenance cost of the infrastructure, which of course should be as sparse as possible. Unfortunately, this need is at odds with the global observability of the system, namely the capability to determine and to reconstruct the position and orientation of the robot. This problem was analysed at a local level (i.e., when the initial state estimate is close enough to the actual one) in different papers [13]–[15]. In a previous work, we have studied the observability problem in a global sense [16] (i.e., requiring convergence of the estimated state to the actual one from any initial position). Using these observability results, we could define a filter structure that has the same performance of the Extended Kalman Filter (EKF) [17], but it is not liable to a partial or wrong knowledge on the noise level affecting the sensors [18].

In this paper, we show a planning strategy that mediates between securing a steady progress toward the goal and keeping localisation uncertainty small enough. The result is obtained through an artificial potential function containing a term related to the goal and a term that accounts for the uncertainty on

the Cartesian position in a given reference frame. The gradient of the potential designed in this way defines, for each point, the correct direction of motion. The amount of motion along the gradient is decided seeking to optimise the uncertainty of the reconstructed angle. The approach relies on a previous work by Salaris et al. [19], in which the Authors propose a motion strategy that maximises the intake of information (quantified through the constructibility Grahamian). The Authors consider a differentially flat continuous-time system, and utilise the point-wise linearised dynamics. Therefore, their technique applies "locally" in a neighbourhood of a given trajectory. On the contrary, taking inspiration from [16], we use a discrete-time formulation, adopt a "global" perspective and restrict our focus on how the estimation uncertainty affect both the Cartesian coordinates and the reconstructed angle.

The paper is organised as follows: Section II describes the background and presents the problem. In Section III, we show how the closed-form expression of the uncertainty can be used in the context of a potential-based motion planning strategy. In Section IV we report several simulation results to substantiate our approach. Finally, we draw our conclusions and outline future research directions in Section V.

II. Background Material and Problem Formulation

In this section, after presenting the dynamic model of the robot, we quickly recall the definition of an observability filter for robot localisation based on a combination of on-board and external range sensors [18]. Then, we will set the background for the paper through a formal definition of the problem.

A. Models

Consider a unicycle robot moving across a space instrumented with m wireless anchor nodes (e.g., based on UWB signals), whose coordinates (X_i, Y_i) are known in a reference frame $\langle W \rangle$. Assuming that the sampling period of the ranging system is T_s, at each time step kT_s, $k \in \mathbb{N}$, the moving agent collects a set of distance measurement data. Such values are grouped together into the vector

$$z_k = \begin{bmatrix} z_{1,\,k} \\ z_{2,\,k} \\ \cdots \\ z_{m,\,k} \end{bmatrix} = \begin{bmatrix} \sqrt{(x_k - X_1)^2 + (y_k - Y_1)^2} \\ \sqrt{(x_k - X_2)^2 + (y_k - Y_2)^2} \\ \cdots \\ \sqrt{(x_k - X_m)^2 + (y_k - Y_m)^2} \end{bmatrix}, \quad (1)$$

where (x_k, y_k) are the Cartesian coordinates of the mid-point of the unicycle wheel axle. Under the customary assumption that the forward v_k and angular ω_k velocities of the vehicle are held constant during each sampling interval $[kT_s, (k+1)T_s]$, it is possible to find the following discrete–time equivalent dynamics for the robot [16], i.e.

$$\begin{aligned} x_{k+1} &= x_k + \Phi_k \cos(\theta_k) - \Psi_k \sin(\theta_k) = x_k + \delta_{x_k}, \\ y_{k+1} &= y_k + \Psi_k \cos(\theta_k) + \Phi_k \sin(\theta_k) = y_k + \delta_{y_k}, \\ \theta_{k+1} &= \theta_k + 2\phi_k, \end{aligned} \quad (2)$$

where

$$\phi_k = \frac{\omega_k}{2} T_s \text{ and } A_k = 2\frac{v_k}{\omega_k} \sin\left(\frac{\omega_k}{2} T_s\right), \quad (3)$$

$\Phi_k = A_k \cos(\phi_k)$ and $\Psi_k = A_k \sin(\phi_k)$. We will exploit the fact that when $\omega_k \to 0$, the A_k coefficient takes its limit value:

$$\lim_{\omega_k \to 0} A_k = \lim_{\omega_k \to 0} 2\frac{v_k}{\omega_k} \sin\left(\frac{\omega_k}{2} T_s\right) = v_k T_s.$$

B. Observability

As stated in [16], the use of $m \geq 3$ non-collinear anchor nodes avoids any ambiguity in estimating any trajectory with $v_k \neq 0$, thus enabling global observability if trilateration or multilateration from the anchors is applied twice in a row when the robot moves between two different nearby positions. Indeed, as known, the Cartesian coordinates (x_k, y_k) of the robot as well as its initial position can be determined from at least three distance values. In particular, given

$$\begin{aligned} z_{i,k}^2 &= (x_k - X_i)^2 + (y_k - Y_i)^2 = \\ &= X_i^2 + x_k^2 + y_k^2 + Y_i^2 - 2X_i x_k - 2Y_i y_k, \end{aligned} \quad (4)$$

with $i = 1, \ldots, m$, by subtracting $z_{i,k}^2$ from $z_{1,k}^2$, i.e. $\Delta_{i,k} = z_{1,k}^2 - z_{i,k}^2$, we get

$$h_k^{(m)} = 2\Sigma^{(m)} \begin{bmatrix} x_k \\ y_k \end{bmatrix} = \begin{bmatrix} \Delta_{2,k} - X_1^2 - Y_1^2 + X_2^2 + Y_2^2 \\ \Delta_{3,k} - X_1^2 - Y_1^2 + X_3^2 + Y_3^2 \\ \vdots \\ \Delta_{m,k} - X_1^2 - Y_1^2 + X_m^2 + Y_m^2 \end{bmatrix}, \quad (5)$$

where

$$\Sigma^{(m)} = \begin{bmatrix} X_2 - X_1 & Y_2 - Y_1 \\ X_3 - X_1 & Y_3 - Y_1 \\ \vdots & \vdots \\ X_m - X_1 & Y_m - Y_1 \end{bmatrix}. \quad (6)$$

Observe that using three non-collinear anchors (5), matrix $\Sigma^{(3)}$ is invertible and produces the planar position (x_k, y_k). Finally, the trajectory angle θ_k can be estimated indirectly from (2) once the pair of values (x_k, y_k) and (x_{k+1}, y_{k+1}) in two consecutive positions are estimated through (5). In particular, if $R(\phi_k)$ denotes the two-dimensional rotation matrix of angle ϕ_k, we have that

$$A_k R(\phi_k) \begin{bmatrix} \cos(\theta_k) \\ \sin(\theta_k) \end{bmatrix} = \begin{bmatrix} x_{k+1} - x_k \\ y_{k+1} - y_k \end{bmatrix}, \quad (7)$$

which finally returns $\theta_k = \arctan\left(\frac{\sin(\theta_k)}{\cos(\theta_k)}\right)$.

C. Observability filter design

Using the global observability analysis described in Section II-B, it is possible to design an *Observability-based Filter* (ObF) for a number of anchors $m \geq 3$, as explained in [18]. The main results are summarised next. The planar coordinates of the robot can be given by the WLS solution

$$\begin{bmatrix} \hat{x}_k \\ \hat{y}_k \end{bmatrix} = \frac{1}{2} (\Sigma^{(m)\,T} N_k^{(m)\,-1} \Sigma^{(m)})^{-1} \Sigma^{(m)\,T} N_k^{(m)\,-1} h_k^{(m)}. \quad (8)$$

where the estimation errors $\widetilde{x}_k = \hat{x}_k - x_k$ and $\widetilde{y}_k = \hat{y}_k - y_k$ are grouped in the position estimation error vector $\xi_k = [\widetilde{x}_k, \widetilde{y}_k]^T$, whose covariance matrix is

$$\Xi_k^{(m)} = (\Sigma^{(m)^T} N_k^{(m)^{-1}} \Sigma^{(m)})^{-1} = \begin{bmatrix} \sigma_{x,k}^2 & \sigma_{xy,k} \\ \sigma_{xy,k} & \sigma_{y,k}^2 \end{bmatrix}. \quad (9)$$

The matrix weighting the covariances is given by

$$N_k^{(m)} = \sigma_\rho^2 \begin{bmatrix} z_{1,\,k}^2 + z_{2,\,k}^2 & z_{1,\,k}^2 & \cdots & z_{1,\,k}^2 \\ z_{1,\,k}^2 & z_{1,\,k}^2 + z_{3,\,k}^2 & \cdots & z_{1,\,k}^2 \\ \vdots & & \ddots & \vdots \\ z_{1,\,k}^2 & z_{1,\,k}^2 & \cdots & z_{1,\,k}^2 + z_{m,\,k}^2 \end{bmatrix}, \quad (10)$$

where the ranging uncertainty $\tilde{z}_{i,k}$ is assumed to be zero-mean, white, Gaussian and with variance σ_ρ^2. As a result, following closed-form expressions of the elements of (9) can be obtained, i.e.

$$\begin{aligned} \sigma_{x,k}^2 &= \frac{\sigma_\rho^{2m-4}}{g_k} \sum_{(i_1,i_2)\in\mathcal{I}} \left(\prod_{j\in\mathcal{J}} z_{j,k}^2 \right) (Y_{i_1} - Y_{i_2})^2, \\ \sigma_{xy,k} &= \frac{\sigma_\rho^{2m-4}}{g_k} \sum_{(i_1,i_2)\in\mathcal{I}} \left(\prod_{j\in\mathcal{J}} z_{j,k}^2 \right) (X_{i_1} - X_{i_2})(Y_{i_1} - Y_{i_2}), \\ \sigma_{y,k}^2 &= \frac{\sigma_\rho^{2m-4}}{g_k} \sum_{(i_1,i_2)\in\mathcal{I}} \left(\prod_{j\in\mathcal{J}} z_{j,k}^2 \right) (X_{i_1} - X_{i_2})^2. \end{aligned} \quad (11)$$

Consider that, in the expressions above,

$$g_k = |\Sigma^{(m)^T} N_k^{(m)^{-1}} \Sigma^{(m)}| |N_k^{(m)}|,$$

(with $|M|$ denoting the determinant of a square matrix M), while the set $\mathcal{I}$ in (9) comprises all the pairs of two anchors without replacements out of the m anchors. Thus, the number of elements in $\mathcal{I}$ is $\frac{m(m-1)}{2}$ and i_1 and i_2 denote the first and the second element of the pair. Moreover, if we define $\mathcal{J} = \{1, \ldots, m\}/\{i_1, i_2\}$, the number of elements of $\mathcal{J}$ is $m-2$. Notice that the position estimation error sequence ξ_k has a zero mean, thus ensuring that the filter based on (8) is unbiased. As far as robot orientation estimation is considered instead, we have that

$$\hat{\theta}_k = \arctan\left(\frac{\cos(\overline{\phi}_k)(\hat{y}_{k+1} - \hat{y}_k) - \sin(\overline{\phi}_k)(\hat{x}_{k+1} - \hat{x}_k)}{\sin(\overline{\phi}_k)(\hat{y}_{k+1} - \hat{y}_k) + \cos(\overline{\phi}_k)(\hat{x}_{k+1} - \hat{x}_k)} \right), \quad (12)$$

that approximated to the first order gives $\hat{\theta}_k \approx \theta_k + \widetilde{\theta}_k$ with variance

$$\sigma_{\theta_k}^2 = \frac{\sigma_\omega^2 T_s^2}{4} + \frac{1}{A_k^4} B_k (\Xi_k^{(m)} + \Xi_{k+1}^{(m)}) B_k^T, \quad (13)$$

where $B_k = [\delta_{y_k}, -\delta_{x_k}]$, $\delta_{x_k} = x_{k+1} - x_k$, $\delta_{y_k} = y_{k+1} - y_k$, $A_k^2 = \delta_{x_k}^2 + \delta_{y_k}^2$ and Ξ_k is reported in (9). Since to design a dynamic estimator, we need the orientation angle estimate at the same time instant of the last collected measurement, i.e. at $(k+1)T_s$, we can exploit the vehicle dynamic (2) (although affected by uncertainty) to propagate the estimate one step forward. Thus, the uncertainty contributions $\widetilde{\theta}_{k+1} = \widetilde{\theta}_k + \eta_k T_s$ affecting $\hat{\theta}_{k+1}$ also exhibit zero mean and variance $\sigma_{\theta_{k+1}}^2 = \sigma_{\theta_k}^2 + T_s^2 \sigma_\omega^2$. Finally, the estimated state $\hat{s}_{k+1} = [\hat{x}_{k+1}, \hat{y}_{k+1}, \hat{\theta}_{k+1}]^T$ is affected by an uncertainty contribution $[\xi_{k+1}^T, \widetilde{\theta}_{k+1}]^T$, whose covariance matrix is

$$\Gamma_{k+1} = \begin{bmatrix} \Xi_{k+1}^{(m)} & \Xi_{k+1}^{(m)} B_{k+1}^T \\ B_{k+1} \Xi_{k+1}^{(m)} & \sigma_{\theta_{k+1}}^2 \end{bmatrix}. \quad (14)$$

D. Problem formulation

Equation (9) defines the position uncertainty as a function of matrix $N_k^{(m)}$, which in turn depends on the Cartesian coordinates (x_k, y_k), and so does the orientation standard uncertainty given by the square root of (13). Given a final goal position, the objective of this paper is to identify the trajectory that allows the robot to reach the goal, while reducing the localisation uncertainty as much as possible. A good way to quantify the latter is by using the trace of the matrix Γ_{k+1} in (14). Thereby the desired motion plan is to seek a sequence of points such that the next point to reach from the current position reduces both the distance to the goal and the trace of Γ_{k+1}.

III. Minimising uncertainty through motion planning

In this section, we will present the motion planning synthesis to solve the problem at hand. Specifically, we will adopt a planning solution based on Artificial Potential Fields (APF) [20]. The idea is to define a potential function having a minimum on the goal while accounting for localisation uncertainty, i.e.

$$V_{tot}(x, y) = V_{goal}(x, y) + \tilde{V}(x, y), \quad (15)$$

where $V_{goal}(x, y) = \alpha[(x - X_{goal})^2 + (y - Y_{goal})^2]$ (with α being a tuning factor), and the term $\tilde{V}(x, y)$ accounts for the uncertainty contributions. At each time step k, the robot navigation algorithm

1) Estimates the robot position $(\hat{x}_k, \hat{y}_k)$;
2) Computes the gradient $\nabla_{x_k,\,x_k} V_{tot}(\hat{x}_k,\, \hat{x}_k)$;
3) Set $[x_{k+1}, y_{k+1}]^T = [\hat{x}_k, \hat{x}_k]^T + \gamma \mathbf{u}_k$, where $\mathbf{u}_k$ is the unit vector associated with the gradient direction;
4) Determines the robot linear and angular velocities v_k and ω_k (accounting for their maximum values) so as to approach the desired position (x_{k+1}, y_{k+1}) as closely as possible.

The term $\tilde{V}(x, y)$ is then given by $\text{Tr}\left(\Xi_k^{(m)}\right)$, which in turn results from

$$\text{Tr}\left(\Xi_k^{(m)}\right) = \text{Tr}\left((\Sigma^{(m)^T} N_k^{(m)^{-1}} \Sigma^{(m)})^{-1} \right) \propto \text{Tr}\left(N_k^{(m)}\right),$$

. In fact, a direct proportionality exist between the variance of the robot position and the ranging measurements, i.e. from (10) we have

$$\text{Tr}\left(N_k^{(m)}\right) = \sigma_\rho^2 \left[(m-1) z_{1,\,k}^2 + \sum_{i=2}^{m} z_{i,\,k}^2 \right].$$

The computation of the gradient comes as a direct consequence

$$\frac{\partial \mathrm{Tr}\left(N_{k+1}\right)}{\partial x_k} = 2\Bigg[(m-1)(x_k - X_1) + \sum_{i=2}^{m}(x_k - X_i)\Bigg]$$
$$\frac{\partial \mathrm{Tr}\left(N_{k+1}\right)}{\partial y_k} = 2\Bigg[(m-1)(y_k - Y_1) + \sum_{i=2}^{m}(y_k - Y_i)\Bigg].$$

Hence the direction of the gradient of the potential function (15) is given by:

$$\nabla_{x_k,\,y_k} V_{tot} = \begin{bmatrix} 2\left((m-1)(x_k - X_1) + \sum_{i=2}^{m}(x_k - X_i)\right) + 2\alpha(x_k - X_{goal}) \\ 2\left((m-1)(y_k - Y_1) + \sum_{i=2}^{m}(y_k - Y_i)\right) + 2\alpha(y_k - Y_{goal}) \end{bmatrix}^T \tag{16}$$

We now analyse the term related to angular variance $\sigma^2_{\theta_{k+1}}$. Given two consecutive measurements at time k and $k+1$, this term derives from (13) and it is given by

$$\sigma^2_{\theta_{k+1}} = \frac{5\sigma^2_\omega T_s^2}{4} + \frac{1}{A_k^4} B_k(\Xi_k^{(m)} + \Xi_{k+1}^{(m)})B_k^T,$$

where the first term is constant and the second one is the only directly related to the input values. We first derive the relation between the uncertainties (11) in two consecutive time instants k and $k+1$. To this end, by combining (4) and (2), it results that

$$\begin{aligned} z^2_{i,\,k+1} &= z^2_{i,\,k} + A_k^2 + 2\left[\delta_{x_k}(x_k - X_i) + \delta_{y_k}(y_k - Y_i)\right] = \\ &= z^2_{i,k} + A_k^2 + \Delta z_{i,k}, \end{aligned} \tag{17}$$

where we made explicit that the change of range is directly proportional to the projection of the displacement of the robot at time k along the line joining the robot position and the anchor position, i.e.

$$\Delta z_{i,k} = 2\left\langle \begin{bmatrix} x_k - X_i \\ y_k - Y_i \end{bmatrix}, \begin{bmatrix} \delta_{x_k} \\ \delta_{y_k} \end{bmatrix} \right\rangle.$$

Recalling that $A_k^2 = \delta^2_{x_k} + \delta^2_{y_k}$, it is then possible to plug (17) into (11) and retrieve a nice dependence of $\Xi_{k+1}^{(m)}$ on $\Xi_k^{(m)}$, δ_{x_k} and δ_{y_k}. If we set $[\delta_{x_k}, \delta_{y_k}]^T = \gamma \mathbf{u}_k$, the uncertainty $\sigma^2_{\theta_{k+1}}$ becomes a function of γ. Indeed, by defining

$$\Theta(\Xi_k^{(m)}, \gamma\mathbf{u}_k) = \Xi_k^{(m)} + \Xi_{k+1}^{(m)} = \begin{bmatrix} \underline{\sigma}^2_{x,k+1} & \underline{\sigma}_{xy,k+1} \\ \underline{\sigma}_{xy,k+1} & \underline{\sigma}^2_{y,k+1} \end{bmatrix},$$

where $\underline{\sigma}^2_{x,k+1} = \sigma^2_{x,k+1} + \sigma^2_{x,k}$, $\underline{\sigma}^2_{y,k+1} = \sigma^2_{y,k+1} + \sigma^2_{y,k}$ and $\underline{\sigma}_{xy,k+1} = \sigma_{xy,k+1} + \sigma_{xy,k}$, we finally have that $\sigma^2_{\theta_{k+1}}(\gamma)$. Therefore, γ in our gradient based descent will be chosen as $\gamma = \mathrm{argmin}\, \sigma^2_{\theta_{k+1}}(\gamma)$.

A. An alternative of the $\tilde{V}$ artificial potential

For the sake of comparison, as an alternative to minimising the trace of $N_{k+1}^{(m)}$, we also consider the minimisation of the Geometric Dilution of Precision (GDOP), which is inspired by the GPS localisation problem and expresses the ranging-based position estimation uncertainties considering only the geometry of the UWB anchors deployment [21]. To refer to the two methods, we use acronyms TM (Trace minimisation) in the former case and GM (GDOP minimisation) in the latter case. Denoting with H_k the Jacobian of (1), whose i-th row is then given by

$$H_{i,k} = \begin{bmatrix} \frac{x_k - X_i}{z_{i,k}} & \frac{y_k - Y_i}{z_{i,k}} \end{bmatrix} = \begin{bmatrix} \cos(\eta_i) & \sin(\eta_i) \end{bmatrix},$$

and where $\eta_i = \arctan(\frac{y_k - Y_i}{x_k - X_i})$, the best linear unbiased estimation (BLUE) of the target position yields the following covariance matrix $\Xi_k^{(m)} = (H_k^T R^{-1} H_k)^{-1} = \frac{1}{\sigma_\rho^2}(H_k^T H_k)^{-1}$, in which $R = \sigma_\rho^2 I_m$ is the covariance of ranging measurements and I_m is the identity matrix of order m. Since the GDOP depends only on geometric features and not on the actual ranging uncertainty contributions [21], it is implicitly assumed that $\sigma_\rho^2 = 1$, which yields the following potential field of the uncertainties

$$\tilde{V}(x_k, y_k) = \sqrt{\mathrm{Tr}\left(H_k^T H_k^{-1}\right)}.$$

To determine the gradient of the GDOP, we first notice that

$$H_k^T H_k = \begin{bmatrix} \sum_{i=1}^m \cos(\eta_i)^2 & \sum_{i=1}^m \cos(\eta_i)\sin(\eta_i) \\ \sum_{i=1}^m \cos(\eta_i)\sin(\eta_i) & \sum_{i=1}^m \sin(\eta_i)^2 \end{bmatrix}$$

and, hence, by simple algebraic manipulations we obtain that

$$\tilde{V}(x_k, y_k) = \sqrt{\frac{m}{\sum_{i=1}^{m-1}\sum_{j=i+1}^{m}\sin^2(\eta_i - \eta_j)}} = \sqrt{\frac{m}{\varphi}}.$$

By defining $\delta_{\eta_{i,j}} = \eta_i - \eta_j$, we finally have

$$\begin{aligned} \frac{\partial \tilde{V}(x_k, y_k)}{\partial x_k} &= -\frac{\sqrt{m}}{\varphi\sqrt{\varphi}}\Bigg[\sum_{i=1}^{m-1}\sum_{j=i+1}^{m}\sin(\delta_{\eta_{i,j}})\cos(\delta_{\eta_{i,j}}) \\ &\qquad + \frac{y_k - Y_i}{z^2_{i,k}} - \frac{y_k - Y_j}{z^2_{j,k}}\Bigg], \\ \frac{\partial \tilde{V}(x_k, y_k)}{\partial y_k} &= -\frac{\sqrt{m}}{\varphi\sqrt{\varphi}}\Bigg[\sum_{i=1}^{m-1}\sum_{j=i+1}^{m}\sin(\delta_{\eta_{i,j}})\cos(\delta_{\eta_{i,j}}) \\ &\qquad + \frac{x_k - X_i}{z^2_{i,k}} - \frac{x_k - X_j}{z^2_{j,k}}\Bigg]. \end{aligned} \tag{18}$$

We can therefore plug (18) into (16) and then proceed with the optimisation of both position and orientation, as described previously.

IV. Simulation results

The performance of the proposed approach is investigated through a several simulations. In all the proposed scenarios, both the wheels displacement and UWB ranging measurements are sampled with period $T_s = 0.1$ s. The uncertainty contributions of robot linear and angular velocities v_k and ω_k are assumed to be white and normally distributed, with zero-mean and standard deviations ranging in $\sigma_v \in [0.001,\ 0.2]$ m/s and $\sigma_\omega \in [0.001,\ 0.2]$ rad/s, respectively. The UWB ranging measurements are instead affected by normally distributed, zero-mean and white uncertainty contributions with standard deviations included in the interval $\sigma_\rho \in [0.01,\ 0.1]$ m. The values of $\tilde{V}(x_k, y_k)$ for GM and TM optimisation using $m = 3$ TOA anchors placed in two different ways are depicted in

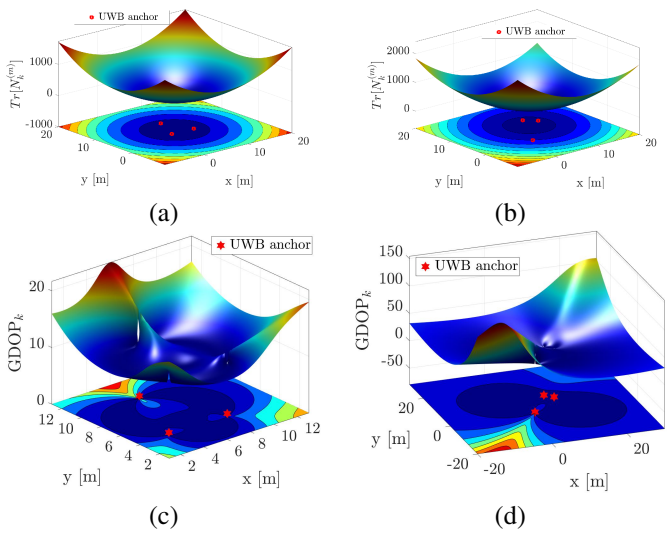

Fig. 1. Representation of the $\tilde{V}(x_k, y_k)$ for TM (a,b) and GM (c,d) optimisations calculated over the entire simulation area. Two different setups of $m = 3$ TOA anchors are adopted in (a,c) and (b,d), respectively.

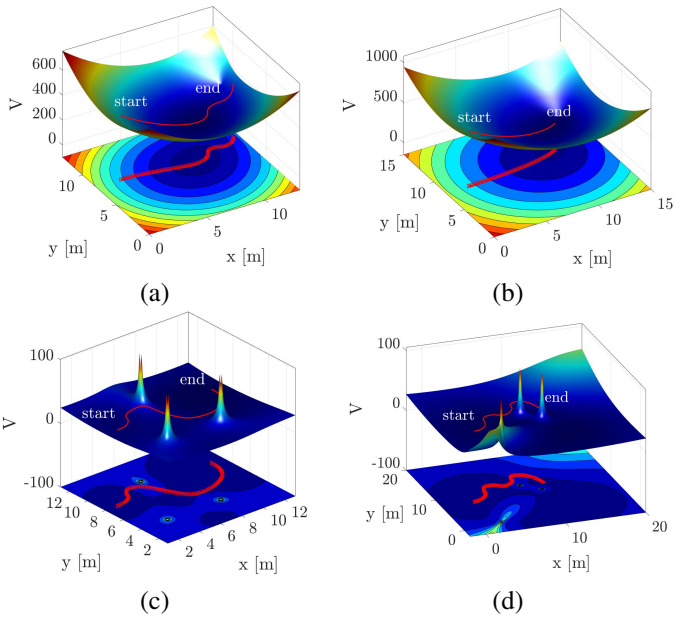

Fig. 2. Sample controlled trajectories for the TM (a,b) and the GM (c, d) in the two scenarios depicted in Figure 1.

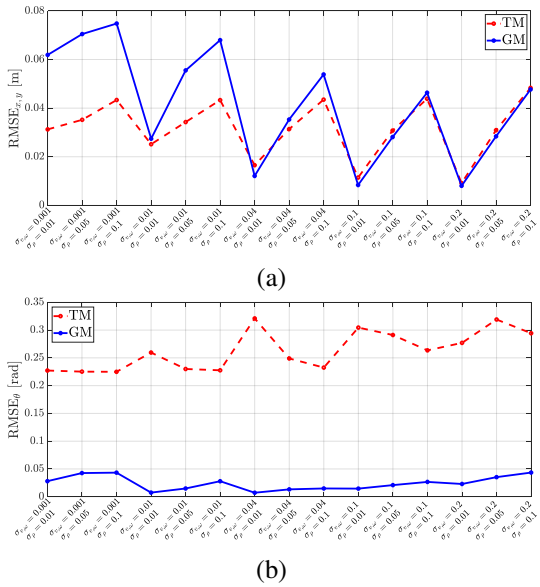

Fig. 3. Position (a) and orientation (b) RMSE for the TM (dashed) and the GM (solid) approaches with different velocity uncertainties (we assume $\sigma_{v\omega} = \sigma_v = \sigma_\omega$) and different ranging uncertainties σ_ρ for the anchor configuration of Figure 1-a,c.

Fig. 1. The expression of Tr $\left(N_k^{(m)}\right)$ in the TM case returns a smooth paraboloid regardless of anchor position (Figure 1-a,b), wheres the GDOP function yields a complicated error surface (Figure 1-c,d), which confirms the benefits of the proposed approach.

As to the trajectories of the robot, once the total APF in (15) is optimised and the gradient direction $\gamma \mathbf{u}_k$ determined, we define a simple control law using (2), thus reverting

$$\gamma \mathbf{u}_k = \begin{bmatrix} \Phi_k \cos(\theta_k) - \Psi_k \sin(\theta_k) \\ \Psi_k \cos(\theta_k) + \Phi_k \sin(\theta_k) \end{bmatrix}.$$

A qualitative analysis of the trajectories obtained with the described approach in the cases depicted in Fig. 1, is shown in Fig. 2. In this examples the initial configuration is placed in $s_i = [2\text{ m}, 8\text{ m}, 0\text{ rad}]$, while the end point position is set as $s_e = [12\text{ m}, 10\text{ m}]$. The final orientations for the TM and the GM solutions is different since it is reached from two different trajectories. In the former case, the final orientation θ is 1.89 rad and 0.7 rad for the first and second configuration, respectively, while for the GM the final orientations are 2.89 rad and -2.79 rad, respectively.

For a quantitative comparison, we carried out a Monte Carlo analysis with 15000 trials, i.e. 1000 trials over 15 different noise conditions, and with the aforementioned initial and final configurations. The two different anchor configurations in Figure 1 are considered. The Root Mean Squared Error (RMSE) of the vehicle localisation is considered and reported in Figures 3 and 4 for the two configurations. It can be noticed that the GM yields better results in orientation, which are more evident in the first configuration of Figure 1-a,c, which is actually optimised for the GDOP since the configuration is symmetric (i.e., the vertices of an equilateral triangle). However, worse position RMSE (i.e. the square root of the mean of $\|\xi_k\|$, that is the norm of the position estimation error) can be noticed, even in the more favourable conditions. Another important result of the analysis is that when the uncertainties grow, the difference between the two approaches actually equalises, except for the orientation in the first configuration. We can then conclude that the TM tends to be a very effective solution compared to the GDOP, mainly due to the simplicity of the optimisation step that stems from the simple paraboloid shape.

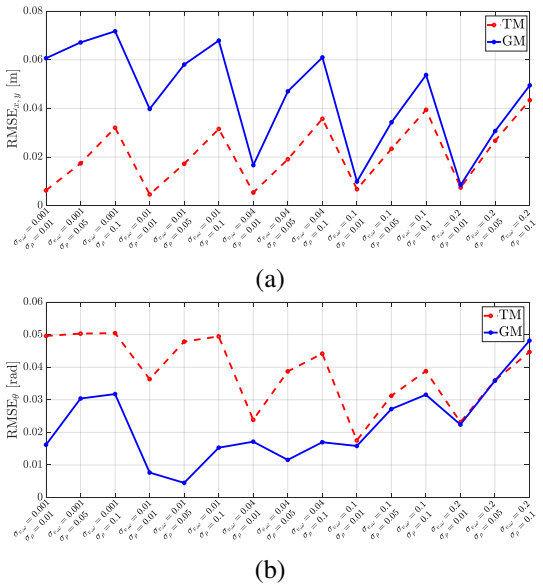

(a)

(b)

Fig. 4. Position (a) and orientation (b) RMSE for the TM (dashed) and the GM (solid) approaches with different velocity uncertainties (we assume $\sigma_{v\omega} = \sigma_v = \sigma_\omega$) and different ranging uncertainties σ_ρ for the anchor configuration of Figure 1-b,d.

V. Conclusions

We have shown a motion planning solution for a mobile robot that strikes a good compromise between a steady progress toward the goal and the localisation accuracy achieved along the way. The potential field-like approach synthesises a path that limits the uncertainty growth using directly the derived closed form of the estimation error covariance matrix accounting for motion and measurement uncertainties. Many problems remain open for future investigation. Three of them are worth mentioning: 1. replacing our two steps control strategy (i.e., estimating the gradient using the uncertainty on the Cartesian components and then estimating the step size using angular uncertainty) with a one step solution in which Cartesian and angular uncertainties are considered at the same time, 2. applying the same ideas to reduce the uncertainty on the position of the anchor (i.e., the mapping problem), which in this paper are assumed perfectly known, 3. extending the application of these ideas to a broader class of systems (e.g., car-like, unicycle with trailers, quadrotors, etc.).

References

[1] K. Cheok, M. Radovnikovich, P. Vempaty, G. Hudas, J. Overholt, and P. Fleck, "UWB tracking of mobile robots," in *Proc. IEEE International Symposium on Personal Indoor and Mobile Radio Communications (PIMRC)*, Instambul, Turkey, Sep. 2010, pp. 2615–2620.

[2] P. Chen, Y. B. Xu, L. Chen, and Z. A. Deng, "Survey of WLAN fingerprinting positioning system," *Applied Mechanics and Materials*, vol. 380, pp. 2499–2505, Aug. 2013.

[3] A. Motroni, P. Nepa, V. Magnago, A. Buffi, B. Tellini, D. Fontanelli, and D. Macii, "SAR-based Indoor Localization of UHF-RFID Tags via Mobile Robot," in *International Conference on Indoor Positioning and Indoor Navigation (IPIN)*. Nantes, France: IEEE, Sept. 2018, pp. 1–8.

[4] P. Nazemzadeh, F. Moro, D. Fontanelli, D. Macii, and L. Palopoli, "Indoor Positioning of a Robotic Walking Assistant for Large Public Environments," *IEEE Trans. on Instrumentation and Measurement*, vol. 64, no. 11, pp. 2965–2976, Nov 2015.

[5] B. Dzodzo, L. Han, X. Chen, H. Qian, and Y. Xu, "Realtime 2D code based localization for indoor robot navigation," in *Proc. IEEE Int. Conference on Robotics and Biomimetics (ROBIO)*, Shenzhen, China, Dec. 2013, pp. 486–492.

[6] V. Magnago, L. Palopoli, A. Buffi, B. Tellini, A. Motroni, P. Nepa, D. Macii, and D. Fontanelli, "Ranging-free UHF-RFID Robot Positioning through Phase Measurements of Passive Tags," *IEEE Trans. on Instrumentation and Measurement*, vol. 69, no. 5, pp. 2408–2418, May 2020.

[7] P. Nazemzadeh, D. Fontanelli, D. Macii, and L. Palopoli, "Indoor Localization of Mobile Robots through QR Code Detection and Dead Reckoning Data Fusion," *IEEE/ASME Transactions on Mechatronics*, vol. 22, no. 6, pp. 2588–2599, Dec. 2017.

[8] M. J. Gallant and J. A. Marshall, "Two-dimensional axis mapping using LiDAR," *IEEE Trans. on Robotics*, vol. 32, no. 1, pp. 150–160, Feb. 2016.

[9] Y. Zhou, Jun Li, and L. Lamont, "Multilateration localization in the presence of anchor location uncertainties," in *2012 IEEE Global Communications Conferenc (GLOBECOM)*, 2012, pp. 309–314.

[10] D. Macii, A. Colombo, P. Pivato, and D. Fontanelli, "A Data Fusion Technique for Wireless Ranging Performance Improvement," *IEEE Trans. on Instrumentation and Measurement*, vol. 62, no. 1, pp. 27–37, Jan. 2013.

[11] D. Giovanelli, E. Farella, D. Fontanelli, and D. Macii, "Bluetooth-based Indoor Positioning through ToF and RSSI Data Fusion," in *International Conference on Indoor Positioning and Indoor Navigation (IPIN)*. Nantes, France: IEEE, Sept. 2018, pp. 1–8.

[12] DecaWave, "DW1000 Data Sheet," 2016.

[13] G. P. Huang, N. Trawny, A. I. Mourikis, and S. I. Roumeliotis, "Observability-based consistent ekf estimators for multi-robot cooperative localization," *Autonomous Robots*, vol. 30, no. 1, pp. 99–122, 2011.

[14] G. L. Mariottini, G. Pappas, D. Prattichizzo, and K. Daniilidis, "Vision-based localization of leader-follower formations," in *Proceedings of the 44th IEEE Conference on Decision and Control*. IEEE, 2005, pp. 635–640.

[15] S. Cedervall and X. Hu, "Nonlinear observers for unicycle robots with range sensors," *IEEE transactions on automatic control*, vol. 52, no. 7, pp. 1325–1329, 2007.

[16] L. Palopoli and D. Fontanelli, "Global Observability Analysis of a Nonholonomic Robot using Range Sensors," in *European Control Conference (ECC)*, San Petersburg, Russia, May 2020.

[17] V. Magnago, P. Corbalán, G. Picco, L. Palopoli, and D. Fontanelli, "Robot Localization via Odometry-assisted Ultra-wideband Ranging with Stochastic Guarantees," in *Proc. IEEE/RSJ International Conference on Intelligent Robots and System (IROS)*. Macao, China: IEEE, Oct. 2019, pp. 1–7, accepted.

[18] L. Palopoli, D. Macii, and D. Fontanelli, "A Positioning Filter based on Uncertainty and Observability Analyses for Nonholonomic Robots," in *Proc. IEEE Int. Instrumentation and Measurement Technology Conference (I2MTC)*. Dubrovnik, Croatia: IEEE, May 2020, pp. 1–6, available online.

[19] P. Salaris, M. Cognetti, R. Spica, and P. R. Giordano, "Online optimal perception-aware trajectory generation," *IEEE Transactions on Robotics*, vol. 35, no. 6, pp. 1307–1322, 2019.

[20] C. W. Warren, "Global path planning using artificial potential fields," in *1989 IEEE International Conference on Robotics and Automation*. IEEE Computer Society, 1989, pp. 316–317.

[21] R. Zekavat and R. M. Buehrer, *Handbook of position location: Theory, practice and advances*. John Wiley & Sons, 2011, vol. 27.